

Inter-Turn Short-Circuit Fault Detection in Synchronous Reluctance Machines, Based on Current Analysis [†]

Kévin Henriques ^{*}, Khaled Laadjal ^{*} and Antonio J. Marques Cardoso ^{*}

CISE–Electromechatronic Systems Research Centre, University of Beira Interior, Calçada Fonte do Lameiro, P–62001-001 Covilhã, Portugal

^{*} Correspondence: kevin.m.henriques@gmail.com (K.H.); laadjal.khaled1991@gmail.com (K.L.); ajmcardoso@ieee.org (A.J.M.C.)

[†] Presented at the 1st International Electronic Conference on Machines and Applications, 15–30 September 2022; Available online: <https://iecma2022.sciforum.net>.

Abstract: Fault diagnosis in electrical drives can be very difficult, especially when the input data comes from an operating electrical machine. The occurrence of Inter-Turns Short-Circuit (ITSC) fault is one of the most dangerous electrical machine failures, and if these are not detected at an early stage of development, they can result in serious consequences, both in terms of repair cost and safety. In this context, an effective off-line approach for diagnosing ITSC fault is proposed, which is based on the computation of a specific severity indicator. This does not require the determination of motor parameters and just involves the use of current sensors. Several tests were performed on a Synchronous Reluctance Machine (SynRM), for various operating conditions (healthy and faulty). The obtained results confirm the effectiveness of the proposed technique for diagnosing ITSC faults, with high reliability, rapidity, and accuracy.

Keywords: Inter-Turn Short-Circuit Fault; Synchronous Reluctance Machine; Current Analysis; Zero Sequence of the Current

Citation: Henriques, K.; Laadjal, K.; Marques Cardoso, A.J. Inter-Turn Short-Circuit Fault Detection in Synchronous Reluctance Machines, Based on Current Analysis. *Eng. Proc.* **2022**, *4*, x. <https://doi.org/10.3390/xxxxx> Published: 15 September 2022

Publisher’s Note: MDPI stays neutral with regard to jurisdictional claims in published maps and institutional affiliations.



Copyright: © 2022 by the authors. Submitted for possible open access publication under the terms and conditions of the Creative Commons Attribution (CC BY) license (<https://creativecommons.org/licenses/by/4.0/>).

1. Introduction

Nowadays, electrical machines are part of the day-to-day life of society, providing convenience and comfort in various domestic and industrial applications, enabling technological development and growth. Since then, the need for them to remain in operation for prolonged periods of time has increased, and consequently, motor malfunctions have started to appear, thus the need to diagnose malfunctions occurring in them has increased.

In the case of the motor under study, the Synchronous Reluctance Motor (SynRM), the most common faults are found in the rotor circuit as inter-turn circuit faults. In this way, three groups of methods are presented in the literature for the detection of this faults, which are analytical model-based, signal processing method and knowledge-based method [1].

Just like that, analytical model-based methods need the models to be accurate, as in [2–4]. These methods are based in the comparison between a simulation model and an experimental model.

The signal processing analyses quantitatively the characteristics of a specific motor signal or make the observation of specific harmonics, as in [5,6]. Where the analysis of the current and voltage signals is obtained from the motor, or the application of the Fast Fourier Transform (FFT) is performed to obtain a spectrum that varies according to the operating conditions of the motor.

Finally, the knowledge-based approach uses artificial intelligence techniques, for approaches through knowledge, as in [7–9].

In this way, this paper proposes a signal processing method, that consists of acquiring the motor input currents and voltages. Then, the Fortescue Transform (FT) is applied off-line to obtain the Zero Sequence of the Current (ZSC) and after that it is applied the FFT to obtain the spectrum of the current I_a and ZSC. With this technique it is possible to detect the occurrence of the ITSC from the current and voltage signals of the three phases. To demonstrate the efficiency of this technique, several experimental tests were carried out in open and closed loop control, with the aim of studying the behavior of the symmetrical components of the current in the presence of ITSC, under load variations.

2. Theoretical Context

In this chapter, the motor components are presented analytically for healthy and faulty operating conditions.

2.1. Healthy Motor

For a three-phase SynRM fed by a three-phase balanced voltage supply, which contains Time Harmonics (TH). The general equations for the three-phase currents are given by [10,11]:

$$\begin{cases} i_a(t) = \hat{i}_{TH}^v \cos(v\omega_s t) + \hat{i}_{RSH}^v \cos[(v\omega_s \mp kN_r \omega_r)t] \\ i_b(t) = \hat{i}_{TH}^v \cos(v\omega_s t - 2\pi/3) + \hat{i}_{RSH}^v \cos[(v\omega_s \mp kN_r \omega_r)t - 2\pi/3] \\ i_c(t) = \hat{i}_{TH}^v \cos(v\omega_s t - 4\pi/3) + \hat{i}_{RSH}^v \cos[(v\omega_s \mp kN_r \omega_r)t - 4\pi/3] \end{cases} \quad (1)$$

where $v=1,3,5,\dots$, is the order of the TH, \hat{i}_{TH}^v represents the amplitude of the TH, \hat{i}_{RSH}^v is the amplitude of the slot harmonic (RSH) as a function of v , N_r is the number of slots of the rotor, ω_r is the rotor speed, p is the number of pole pairs and k is a integer.

TH happen due to the power supply, while RSH are the result of the discrete distribution in the rotor slots. However, the SynRM, even in a healthy state, contains certain levels of both static and dynamic residual eccentricities. These are known as Eccentricity Fault Harmonics (EFH) [10,11]. Thus, the frequencies can be expressed as follows:

$$f_{EFH} = (vf_s \pm kf_r) \quad (2)$$

In this way, the stator currents of a SynRM in a healthy state, contain spectral components, which are related to the residual mixed eccentricity fault. Hence, it is possible to write:

$$\begin{cases} i_a(t) = \hat{i}_{TH}^v \cos(v\omega_s t) + \hat{i}_{EFH}^v \cos[(v\omega_s \mp k\omega_r)t] + \hat{i}_{RSH}^v \cos[(v\omega_s \mp kN_r \omega_r)t] \\ i_b(t) = \hat{i}_{TH}^v \cos(v\omega_s t - 2\pi/3) + \hat{i}_{EFH}^v \cos[(v\omega_s \mp k\omega_r)t - 2\pi/3] + \hat{i}_{RSH}^v \cos[(v\omega_s \mp kN_r \omega_r)t - 2\pi/3] \\ i_c(t) = \hat{i}_{TH}^v \cos(v\omega_s t - 4\pi/3) + \hat{i}_{EFH}^v \cos[(v\omega_s \mp k\omega_r)t - 4\pi/3] + \hat{i}_{RSH}^v \cos[(v\omega_s \mp kN_r \omega_r)t - 4\pi/3] \end{cases} \quad (3)$$

Being \hat{i}_{EFH}^v the amplitude of EFH as a function of v , and f_r indicates the rotation frequency. The Equation (3) shows that the stator currents for a healthy motor will have an infinite series of three types of harmonics TH, EFH and RSH [10,11].

2.2. Faulty Motor (ITSC)

The existence of a ITSC creates in the phase that it's affected a decrease in the resistance, followed by an increase in the current of the same phase [10,11].

The occurrence of an ITSC induces current harmonics in the stator with frequencies, which is given by:

$$f_{ITSC} = vf_s \mp kf_r \quad (4)$$

in which f_r the rotation frequency, $v=1,3,5,\dots$ and k an integer.

As can be noted this equation is the same as Equation (2). Thus, it is possible to detect a clear ambiguity between the values of the mixed eccentricity and ITSC fault. So, in this

context the effect of an ITSC fault, in other words is the same as shorting a winding, due to these shorter windings the MMF produced is weaker. Furthermore, the current circulating in the short-circuited windings also produces an MMF that is opposite to the main MMF created by the phase windings. Consequently, the new MMF is the subtraction of the MMF induced by the short-circuited turns with the MMF generated by the stator in normal operation.

Therefore, the currents of the stator with ITSC fault, can be given by:

$$\begin{cases} i_a(t) = \hat{i}_{TH}^v|_{SC} \cdot \cos(v\omega_s t) + \hat{i}_{EFH}^v|_{SC} \cos[(v\omega_s \mp k\omega_r)t] + \hat{i}_{RSH}^v|_{SC} \cdot \cos[(v\omega_s \mp kN_r\omega_r)t] \\ i_b(t) = \hat{i}_{TH}^v|_{SC} \cdot \cos(v\omega_s t - 2\pi/3) + \hat{i}_{EFH}^v|_{SC} \cos[(v\omega_s \mp k\omega_r)t - 2\pi/3] + \hat{i}_{RSH}^v|_{SC} \cdot \cos[(v\omega_s \mp kN_r\omega_r)t - 2\pi/3] \\ i_c(t) = \hat{i}_{TH}^v|_{SC} \cdot \cos(v\omega_s t - 4\pi/3) + \hat{i}_{EFH}^v|_{SC} \cos[(v\omega_s \mp k\omega_r)t - 4\pi/3] + \hat{i}_{RSH}^v|_{SC} \cdot \cos[(v\omega_s \mp kN_r\omega_r)t - 4\pi/3] \end{cases} \quad (5)$$

where, $\hat{i}_{TH}^v|_{SC}$, $\hat{i}_{EFH}^v|_{SC}$ and $\hat{i}_{RSH}^v|_{SC}$ are the new amplitudes of TH, EFH and RSH, respectively, as a function of v , after the presence of the short circuit.

3. Definition of the Indicator

3.1. Fast Fourier Transform (FFT)

It is a signal processing method, these methods as discussed earlier include time, frequency, and time-frequency domain analysis approaches [12].

This represents a signal as a combination of multiple sinusoidal functions, clearly shows the frequency distribution of a signal, representing the amplitude and frequency of the components of harmonics, and can be used to define machine malfunctions [13]. Monitoring through spectral analysis of signals consists in performing a simple $x(t)$ transform of a continuous signal over time, thus allowing to describe any signal in the frequency spectrum, the equation that allows this transformation is given by:

$$x(f) = \int_{-\infty}^{+\infty} x(t)e^{-j2\pi ft} dt \quad (6)$$

To perform the analysis of a signal over a finite period, a weighting window is needed, to correct for the finite time effect. Therefore, the frequency accuracy depends on the sampling frequency (f_s) and the number of samples (N), as shown in:

$$\Delta f = \frac{f_s}{N} \quad (7)$$

The resultant of the previous equation is a frequency directly related to the modifications of the amplitudes of the harmonics, due to defects in the machine operation.

3.2. Fortescue Transform (FT)

The indicator is calculated using the FT. This technique consists in transforming an unbalanced system of polyphase vectors, in several balanced systems. Thus, for a three-phase system, an unbalanced set of voltages or currents, can be transformed into two symmetrical three-phase systems with opposite phase sequence (negative and positive). Besides these two, there is still a third set of equal vectors, that is, zero phase sequence.

In this way, applying this transform to three-phase voltages (V_a, V_b, V_c) of a synchronous reluctance motor, results in three symmetrical components: Positive (V_+), Inverse (V_-) and Zero (V_0). These components can be obtained with the following expression [14]:

$$\begin{bmatrix} V_+ \\ V_- \\ V_0 \end{bmatrix} = \frac{1}{3} \begin{bmatrix} 1 & a & a^2 \\ 1 & a^2 & a \\ 1 & 1 & 1 \end{bmatrix} \begin{bmatrix} V_a \\ V_b \\ V_c \end{bmatrix} \quad (8)$$

Then, the FT is applied to calculate the positive and negative sequences required. Figure 1 illustrates a diagram representing the implementation of the technic.

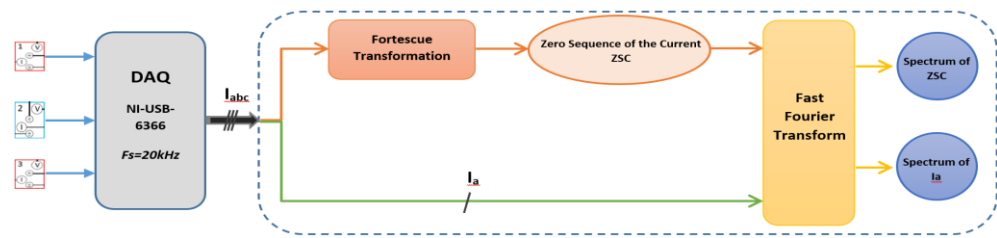


Figure 1. Schematic of the implementation of the proposed technique.

4. Experimental Study

The experimental bench used in the study consists of a SynRM, which has its windings modified by adding tapping's. These make it possible to create ITSCs with different severities of fault. Together with the motor, there is a PMSM as generator and an Industrial Inverter for supply. In Figure 2 shows a general view of the bench and in Table 1 it is presented the parameters of the motor. The voltage and current measurements were made using Tektronix P5200A differential voltage probes, the Tektronix TCPA300 amplifier and Tektronix TCP312 current probes. The corresponding signals were acquired using a NI USB-6366 series data acquisition board with a 20 kHz sampling frequency. These steps were carried out continuously, which enabled the evolution of the indicators and the different magnitudes to be monitored in real time.

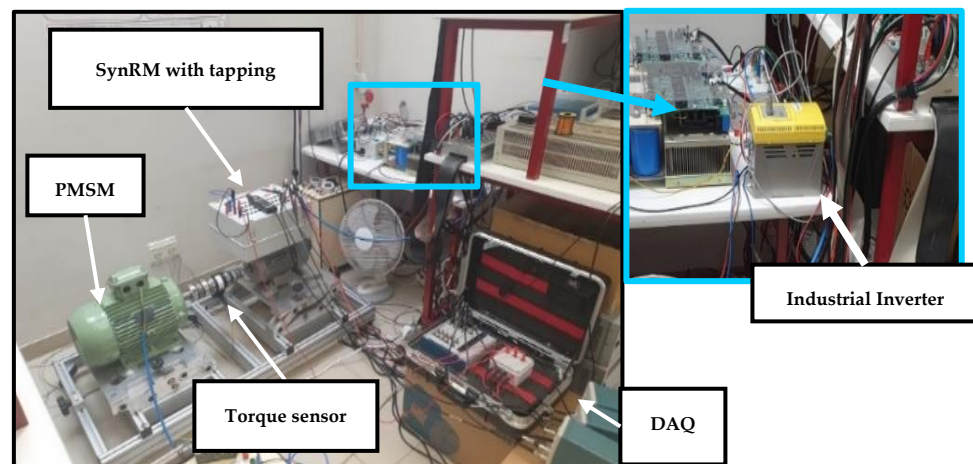


Figure 2. General view of the experimental test bench.

Table 1. SynRM parameters.

| | |
|------------------------------------|-----------|
| Number of poles | 4 |
| Rated Power | 2.2 kW |
| Rated Voltage | 400 V |
| Rated Current | 5.7 A |
| Rated Frequency | 50 Hz |
| Rated Speed | 1500 rpm |
| Rated Inductance of the axis's d/q | 150/25 mH |
| Stator Resistance | 1.71 Ω |

4.1. Open-Loop Control

The experimental results performed with open-loop control are represented in Table 2 that shows the quantitative evaluation of the FFT of the indicators studied. These tests were performed for different scenarios of different severities and loads. As it is possible

to observe, the third harmonic of current and indicator (ZSC) clearly demonstrate the evolution of the fault for different loads, not being affected by load variation.

Table 2. Quantitative values for Ia and ZSC.

| | Load | Faulty State | | | Variation (%) | | | |
|----------------|-------|---------------|----------|----------|---------------|----------|----------|----------|
| | | Healthy State | 12 Turns | 18 Turns | 24 Turns | 12 Turns | 18 Turns | 24 Turns |
| Ia 3Fs | 0 Nm | 0.01909 | 0.05215 | 0.07921 | 0.0985 | 173% | 315% | 416% |
| | 10 Nm | 0.02436 | 0.07129 | 0.1008 | 0.1458 | 193% | 314% | 499% |
| ZSC 3Fs | 0 Nm | 0.01327 | 0.03363 | 0.0512 | 0.06376 | 153% | 286% | 380% |
| | 10 Nm | 0.02087 | 0.04449 | 0.06338 | 0.09313 | 113% | 204% | 346% |

Therefore, Figure 3 shows a graph where it is possible to verify the evolution of the spectrum of the current and the indicator. Analyzing this, it is possible to detect that for both indicators, under different scenarios they show a similar evolution, increasing as the severity increases, proving the effectiveness of this technique to detect faults in open-loop control.

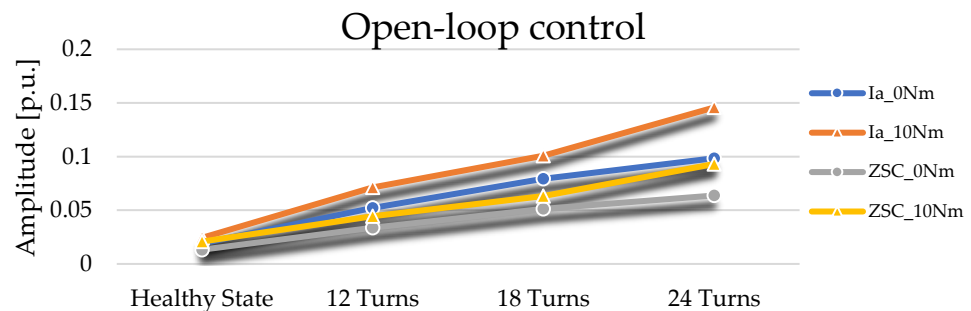


Figure 3. Graph of the evolution of the fault.

4.2. Closed-Loop Control

In this case the tests were performed for a closed-loop control, therefore in Table 3, it is presented a quantitative evolution of the FFT of the indicators. Similar as before, these tests were carried out for different situations with varying loads and severities.

Table 3. Quantitative values for Ia and ZSC.

| | Load | Faulty State | | | Variation (%) | | | |
|----------------|------|---------------|----------|----------|---------------|----------|----------|----------|
| | | Healthy State | 12 Turns | 18 Turns | 24 Turns | 12 Turns | 18 Turns | 24 Turns |
| Ia 3Fs | 0 Nm | 0.0008708 | 0.001283 | 0.001351 | 0.003916 | 47% | 55% | 350% |
| | 4 Nm | 0.00506 | 0.00652 | 0.00727 | 0.007584 | 29% | 44% | 50% |
| ZSC 3Fs | 0 Nm | 0.0012 | 0.001258 | 0.001435 | 0.001829 | 5% | 20% | 52% |
| | 4 Nm | 0.004964 | 0.005263 | 0.005454 | 0.005707 | 6% | 10% | 15% |

In this way, Figure 4 shows a graph where it is possible to verify the evolution of the spectrum of the current and the indicator. By analyzing this, it is possible to see that for both indicators, in different situations, they show a similar evolution, increasing as the severity increases, proving the effectiveness of this technique to detect faults in closed-loop control.

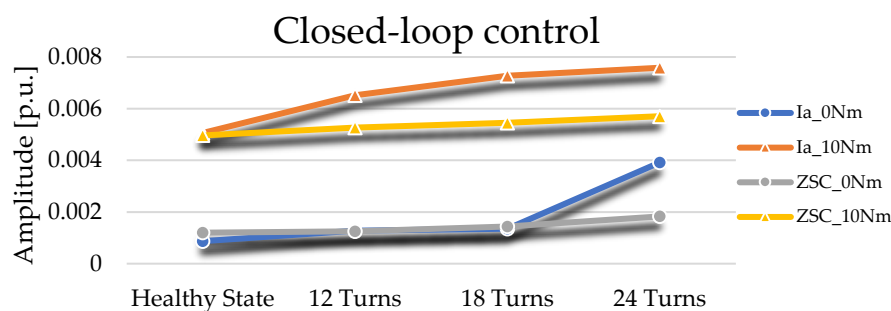


Figure 4. Graph of the evolution of the fault.

5. Conclusions

A new technique, of inter-turn short-circuit fault diagnosis off-line was presented. Based only on the measurement of the three-phase input currents, the proposed strategy uses the FT to calculate the ZSC indicator, afterwards with de FFT the spectrum of the current in phase and the spectrum of ZSC were determined. This allows a fast and reliable detection of an incipient inter-turn short-circuit fault in the SynRM. An analytical study of the SynRM in healthy state and with inter-turn short circuit fault has been presented. The behavior of the proposed indicator has been studied experimentally.

The obtained findings suggest that Ia and ZSC can be regarded as highly reliable indicators for ITSC fault diagnosis in SynRM applications with open-loop control and closed-loop control, and they also validate the accuracy and versatility of the proposed approach. In addition, future research will investigate its online application while considering the occurrence of ITSC faults in different phases, and the sudden variation of the load.

References

- Zhang, Y.; Wang, A.; Guo, B.; Li, H. Diagnosis Methods for Inter-turn Short-circuit Fault Degree of Permanent Magnet Synchronous Motor Stator Winding. In Proceedings of the 2019 6th International Conference on Systems and Informatics (ICSAI), Shanghai, China, 2–4 November 2019; pp. 927–931. <https://doi.org/10.1109/ICSAI48974.2019.9010126>.
- Leboeuf, N.; Boileau, T.; Nahid-Mobarakeh, B.; Clerc, G.; Meibody-Tabar, F. Real-Time Detection of Interturn Faults in PM Drives Using Back-EMF Estimation and Residual Analysis. *IEEE Trans. Ind. Appl.* **2011**, *47*, 2402–2412. <https://doi.org/10.1109/TIA.2011.2168929>.
- Moon, S.; Jeong, H.; Lee, H.; Kim, S.W. Interturn Short Fault Diagnosis in a PMSM by Voltage and Current Residual Analysis With the Faulty Winding Model. *IEEE Trans. Energy Convers.* **2018**, *33*, 190–198. <https://doi.org/10.1109/TEC.2017.2726142>.
- Mahmoudi, A.; Jlassi, I.; Cardoso, A.J.M.; Yahia, K.; Sahraoui, M. Inter-Turn Short-Circuit Faults Diagnosis in Synchronous Reluctance Machines, Using the Luenberger State Observer and Current's Second-Order Harmonic. *IEEE Trans. Ind. Electron.* **2022**, *69*, 8420–8429. <https://doi.org/10.1109/TIE.2021.3109514>.
- Nelson, A.L.; Chow, Mo. Characterization of coil faults in an axial flux variable reluctance PM motor. *IEEE Trans. Energy Convers.* **2002**, *17*, 340–348. <https://doi.org/10.1109/TEC.2002.801730>.
- Neti, P.; Nandi, S. Performance analysis of a reluctance synchronous motor under abnormal operating condition. In Proceedings of the Canadian Conference on Electrical and Computer Engineering 2004 (IEEE Cat. No.04CH37513), Niagara Falls, ON, Canada, 2–5 May 2004; Volume 1, pp. 587–590. <https://doi.org/10.1109/CCECE.2004.1345105>.
- Bouchareb, I.; Bentounsi, A.; Lebaroud, A. Advanced diagnosis strategy for incipient stator faults in synchronous reluctance motor. In Proceedings of the 2015 IEEE 10th International Symposium on Diagnostics for Electrical Machines, Power Electronics and Drives (SDEMPED), Guarda, Portugal, 1–4 September 2015; pp. 110–116. <https://doi.org/10.1109/DEMPED.2015.7303677>.
- Narayan, S.; Kumar, R.R.; Cirrincione, G.; Cirrincione, M. Detection of Stator Fault in Synchronous Reluctance Machines Using Shallow Neural Networks. In Proceedings of the 2021 IEEE Energy Conversion Congress and Exposition (ECCE), Vancouver, BC, Canada, 10–14 October 2021; pp. 1347–1352. <https://doi.org/10.1109/ECCE47101.2021.9595518>.
- Ilhem, B.; Amar, B.; Lebaroud, A. Classification method for faults diagnosis in reluctance motors using Hidden Markov Models. In Proceedings of the 2014 IEEE 23rd International Symposium on Industrial Electronics (ISIE), Istanbul, Turkey, 1–4 June 2014; pp. 984–991. <https://doi.org/10.1109/ISIE.2014.6864746>.

10. Alloui, A.; Laadjal, K.; Sahraoui, M.; Cardoso, A.J.M. Online Inter-Turn Short-Circuit Fault Diagnosis in Induction Motors Operating Under Unbalanced Supply Voltage and Load Variations, Using the STLSP Technique. *IEEE Trans. Ind. Electron.* **2022**, 1–1. <https://doi.org/10.1109/TIE.2022.3172751>.
11. Sahraoui, M.; Ghoggal, A.; Zouzou, S.E.; Benbouzid, M.E. Dynamic eccentricity in squirrel cage induction motors—Simulation and analytical study of its spectral signatures on stator currents. *Simul. Model. Pract. Theory* **2008**, *16*, 1503–1513. <https://doi.org/10.1016/j.simpat.2008.08.007>.
12. Niu, X.; Zhu, L.; Ding, H. New statistical moments for the detection of defects in rolling element bearings. *Int. J. Adv. Manuf. Technol.* **2005**, *26*, 1268–1274. <https://doi.org/10.1007/s00170-004-2109-4>.
13. Rosero, J.A.; Romeral, L.; Cusido, J.; Garcia, A.; Ortega, J.A. On the short-circuiting Fault Detection in a PMSM by means of Stator Current Transformations. In Proceedings of the 2007 IEEE Power Electronics Specialists Conference, Orlando, FL, USA, 17–21 June 2007; pp. 1936–1941. <https://doi.org/10.1109/PESC.2007.4342300>.
14. Laadjal, K.; Sahraoui, M.; Alloui, A.; Cardoso, A.J.M. Three-Phase Induction Motors Online Protection against Unbalanced Supply Voltages. *Machines* **2021**, *9*, 203. <https://doi.org/10.3390/machines9090203>.